Merguerian, Charles; and **Ozdemir, Levent**, 2003, Rock Mass Properties and Hard Rock TBM Penetration Rate Investigations, Queens Tunnel Complex, NYC Water Tunnel #3, Stage 2: p. 1019-1036 *in* Robinson, R.A. and Marquardt, J.M., *eds.,* Rapid Excavation and Tunneling Conference, 2003 Proceedings, 1334 p.

Rock Mass Properties and Hard Rock TBM Penetration Rate Investigations, Queens Tunnel Complex, NYC Water Tunnel #3, Stage 2

ABSTRACT

Between 1996 and 1999, a high-performance Robbins TBM [235-282] excavated a 5 mile long, 23’2” wide, and ~700’ deep tunnel through the subsurface of southwestern Queens. Low penetration rates (~6’/hr [actual] vs. ~9’/hr [anticipated]) resulted from changed rock mass conditions mostly attributable to high-grade metamorphism of the rocks. Over a three-year period, as-built circumferential geologic mapping (scale 1”=10’) and digital imagery of the tunnel, fracture and fault analysis, structural, lithologic, and petrographic studies have shown that the rocks of the Queens Tunnel consist of orthogneiss of mesocratic, leucocratic, and mafic composition. These metaigneous rocks developed coarse-grained fabrics during Grenvillian (~1.0 Ga) granulite facies metamorphism, and retained their nearly anhydrous, poorly foliated character during subsequent high-grade Ordovician deformation. Lacking a penetrative foliation, the coarse granoblastic rock texture and extraordinary garnet content (up to 50% in some zones) together proved an impediment to efficient chip production and resulted in bimodal production of blocks and excessive fines.

TBM excavation of the Queens Tunnel was also hindered by geological conditions that included unexpected lithology and rock fabric orientation, a zone of crosscutting hypabyssal rhyodacite dikes, and unanticipated extent of brittle faults. The dikes and brittle faults produced blocky ground conditions and a collapsing face condition that produced cutter damage and decreased utilization. Such fundamental textural, mineralogic, and lithologic control over hard-rock TBM penetration can be predicted by careful pre-bid geological analysis.

To determine the causes of lower than anticipated TBM performance, a detailed investigation was carried out that included analysis of operational data from the TBM data logger and an extensive laboratory test program on cores retrieved from tunnel walls. Integrated laboratory testing included punch, point load, tensile strength, Cerchar abrasivity, and linear cutting tests, independent petrographic analysis and machine performance analysis. These allied investigations have provided quantification that the rock mass exhibited an unusually high degree of toughness and rock directional properties and established geological causes for decreased TBM penetration rates.

INTRODUCTION

Our combined geological analysis and laboratory testing of the Queens Tunnel Complex provides a case history for poor TBM penetration rates in granulite facies terranes. The Queens Tunnel TBM experienced poor penetration rates and produced excessive fines, the direct result of the lithology, structure, and high-grade metamorphism of the rock mass. In addition to these effects, blocky ground and short stand-up times plagued the construction effort because of the unique internal texture of the gneisses, broad zones of intersecting brittle faults and a suite of internally fractured hypabyssal dike rocks.

Below, we present the results of our allied studies. The report first presents the results of geologic studies of Merguerian, who outlined the geological framework of the as-built tunnel and identified a material change from the anticipated subsurface geology. The second portion presents the results of laboratory testing and analysis by Ozdemir, who provided quantitative explanations for poor penetration and excessive fines, relating them to geological properties encountered during mining.

REGIONAL GEOLOGY AND ANTICIPATION

New York City is situated at the extreme southern terminus of the Manhattan Prong, a northeast-trending, deeply eroded sequence of metamorphosed Proterozoic to Lower Paleozoic rocks that widen northeastward into the crystalline terranes of New England (Rodgers and others 1959; Fisher 1970; Rodgers 1985). Pre-bid and during the early stages of mining, the prediction was that the Queens Tunnel (Figure 1) was to be excavated within the Hartland Formation, a regionally extensive tract of highly aluminous metasedimentary and subordinate metavolcanic rocks of Cambrian to Ordovician age. Despite alignment borings, previously published papers and reports (Baskerville 1989, 1992, 1994; Baskerville and Mose 1989; Hatch and Stanley 1973; Merguerian 1983, 1996; Merguerian and Sanders 1991, 1993) and data from nearby subsurface construction efforts including City Water Tunnel #2, pre-bid subsurface predictions were incorrect. In retrospect, the views of Merrill et al (1902), Berkey (1910, 1933, 1948), and Berkey and Fluhr (1948) were more correct.

Mapping, lithologic, and petrographic studies demonstrated that the lithotypes, metamorphic grade, and lithologic proportions were just not in keeping with the notion that the formation penetrated was the Hartland (Merguerian 1999a, 2000). Focused mineralogical, geochemical, and geochronologic research demonstrated that the Queens Tunnel consisted of a much older, largely metaplutonic orthogneiss complex correlative with the Proterozoic Fordham Gneiss (Brock, Brock and Merguerian 2001; Merguerian 2001; Merguerian, Brock and Brock 2001). Based on these studies, the Queens Tunnel Complex (QTC) was named for garnetiferous intermediate, mafic, and felsic migmatitic gneisses that were exposed during excavation of the Queens Tunnel. The QTC includes compositionally variable high-grade gneiss and amphibolite and younger crosscutting igneous rocks including foliated intrusives, pegmatite, and both mafic- and rhyodacite dikes. Minor metasedimentary units include calc-silicate rock, granofels, and shear-bounded slivers or lenses of biotite-garnet schist that share petrographic characteristics with the Ordovician Walloomsac Schist. As such, these distinctive rocks may be tectonically emplaced within the QTC during younger (presumably Taconian) orogenesis.

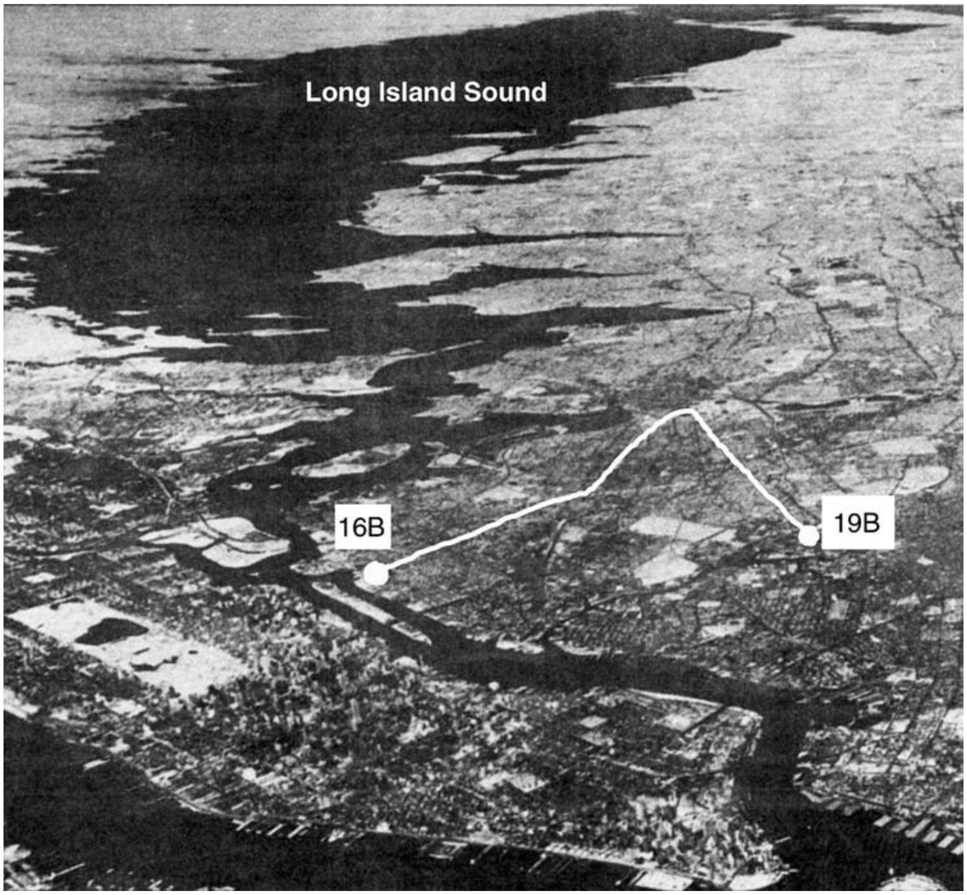

Figure 1 – Oblique northeastward view along the axis of the Long Island Sound. The Sound in a natural boundary (nonconformity) between crystalline rocks of the New England Appalachians (to the left; north) and southward dipping sediments of the Coastal Plain and overlying glacial sediments (to the right; south). The approximate tract of the Queens Tunnel and positions of Shafts 16B and 19B are shown.

GEOLOGICAL INVESTIGATIONS OF THE QUEENS TUNNEL

Mapping Program

Over 100 days of comprehensive mapping of the Queens Tunnel began in May 1998 and was completed by February 2000. A discussion of mapping techniques has been published elsewhere (Merguerian 1999b). To summarize, each cylindrical 100' section of the tunnel was mapped at a scale of 1" = 10', paying careful attention to the structure, lithology, faults, and crosscutting relationships. The field observations that much of the coarse-grained gneiss in the tunnel contained inclusions (screens, xenoliths, and cognate xenoliths) of older rock (Figure 2) and the identification of former intrusive contacts forced the conclusion that the rock mass was largely orthogneiss (metamorphosed intrusive igneous rocks).

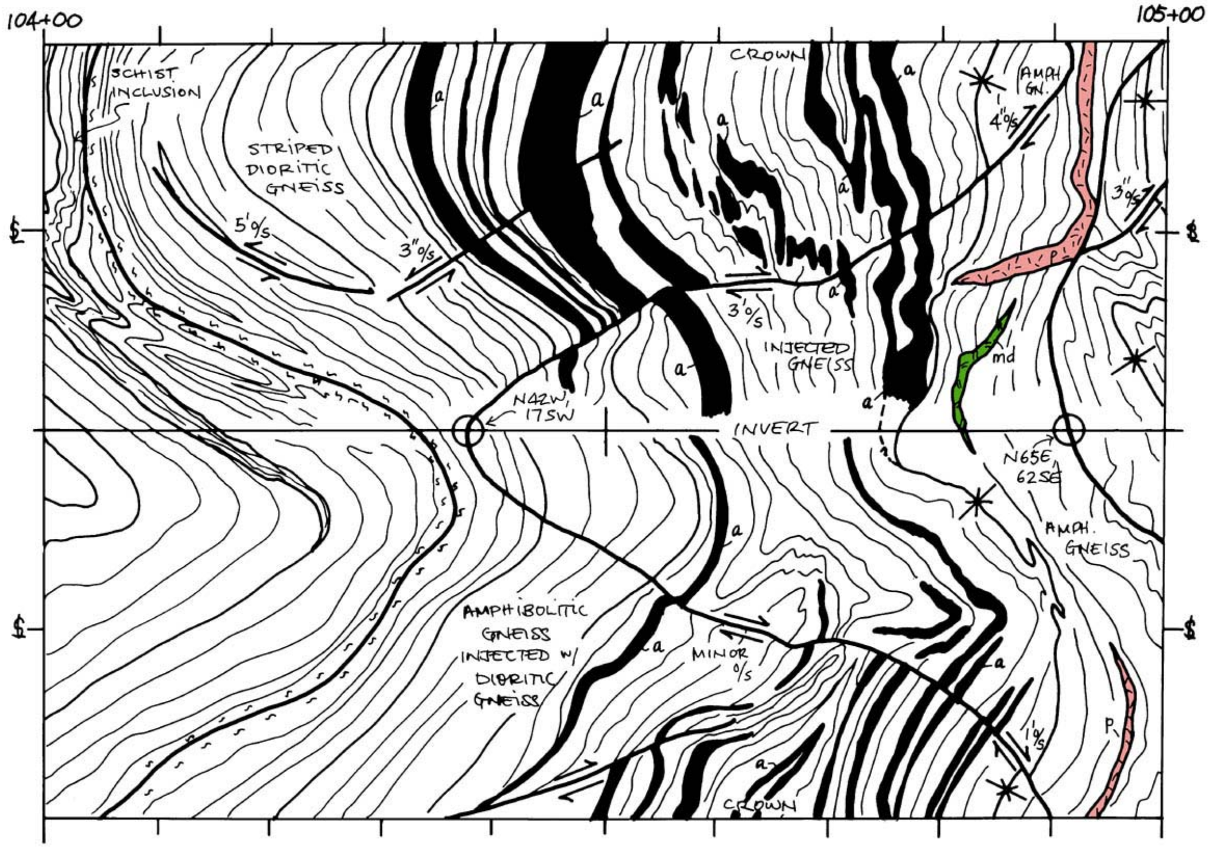

Figure 2 – Map of the Queens Tunnel Complex shows granulite-facies amphibolite gneiss and younger dioritic orthogneiss cut by pegmatite (p) and a mafic dike (md). The amphibolitic gneiss is locally sheared but clearly occurs as inclusions in the dioritic gneiss. A low-angle reverse fault (Group A) oriented N42°W, 17° SW cuts the invert at Station 104+38 (tunnel bearing is N22°E). A younger N65°E, 62°NE brittle fault (Group B) cuts the invert at Station 104+91.

Note: The tunnel invert is shown along the center of the map and the tunnel walls curl upward into a cylinder to join at the crown. Stationing increases from Shaft 19B (to left) toward Shaft 16B. The position of the tunnel springline is shown at the map edge. This map, one of 250 in the Queens Tunnel Map Portfolio, covers 100 running feet of the tunnel. (Original map scale 1"=10'; tunnel diameter 23' 2".)

Mesoscopic and stereomicroscopic examination of 161 Queens Tunnel samples and comparison of the hand specimens to map data demonstrated that a preponderance of the samples were mesocratic (intermediate) to mafic in composition with coarse- to medium grained textures. The rocks were predominately massive metaplutonic rocks exhibiting gneissic structure (orthogneiss) with plagioclase, ortho- and clinopyroxene, garnet, amphibole, and retrograde biotite the principal mineral phases present. Absent were the micas and aluminosilicate mineral phases typical of the predominately schistose Hartland Formation.

Zircons from samples taken from Queens Tunnel Stations 9+45 and 68+15 produced well-defined concordia that yielded isochrons ages of roughly 1.0 Ga (billion years old) for both samples with very minor inheritance. The zircons were from metaigneous rocks with the oldest component about 1.07 Ga and the youngest component older than 949 Ma (million years old). The age data, together with structural field data, lithologic distribution, metamorphic grade, pyroxene+plagioclase+garnet mineralogy, density studies, and geochemical analyses, pointed to a single irrefutable conclusion. The rocks of the Queens Tunnel could not be the Hartland Formation but were closest to the Fordham Gneiss. This result allowed correlation of the QTC with Grenvillian (~1.0 Ga) gneissic rocks found in The Bronx, Westchester County, the Hudson Highlands, and in the Adirondacks massif of New York State.

Borings vs. As-Built Lithology

Analysis of the as-built tunnel maps, rock samples, and thin sections defined the lithotype distribution pattern of the tunnel. The rocks were subdivided into two basic compositional categories – felsic (granitic rock compositions) vs. intermediate- and mafic types (dioritic- and gabbroic rock compositions). The felsic category (29.2%) included granitic, granodioritic, and tonalitic orthogneiss, quartzofeldspathic gneiss, and broad areas of pegmatite and pegmatitic gneiss. The intermediate and mafic categories (66.2%) included metamorphosed dioritic- and gabbroic gneiss, amphibolite ± garnet, mafic dikes, and subordinate biotite schist (Figure 3). Orthogneiss bodies constitute ~30% of the total based on inclusions and cognate xenoliths found during mapping.

Highly fractured rhyodacite dike rocks (2.6%) represent a truly unique non-metamorphosed lithotype for the region. Technically a granitic (felsic) rock, they were not included with the metamorphosed granitic rocks because of their relative youth (~295 Ma), former volcanogenic parentage, and unique rock mass properties. The statistical study concluded that the rocks were far more mafic than the borings indicated, consisting of 66.2% intermediate- and mafic rock types rather than the 40.4% found in the borings. (See Figure 3.) The borings were simply not representative of rocks encountered during tunneling.

Metamorphic History

A thorough investigation of over 150 thin sections proved that most rocks from the Queens Tunnel were metaplutonic in origin that displayed textures and mineral assemblages bearing witness to several episodes of high-grade metamorphism. The bulk of the QTC originated as a vast suite of 1.0 Ga intermediate, mafic and felsic syntectonic plutons, sills, and dikes. These Grenvillian (Proterozoic Y) intrusives cross cut older metasedimentary units and enclose abundant screens, xenoliths, and cognate xenoliths of older orthogneiss. (See Figure 2.) The garnet-clinopyroxene-orthopyroxene-plagioclase assemblages indicate that metamorphism occurred in the high-pressure granulite facies of Spear (1993).

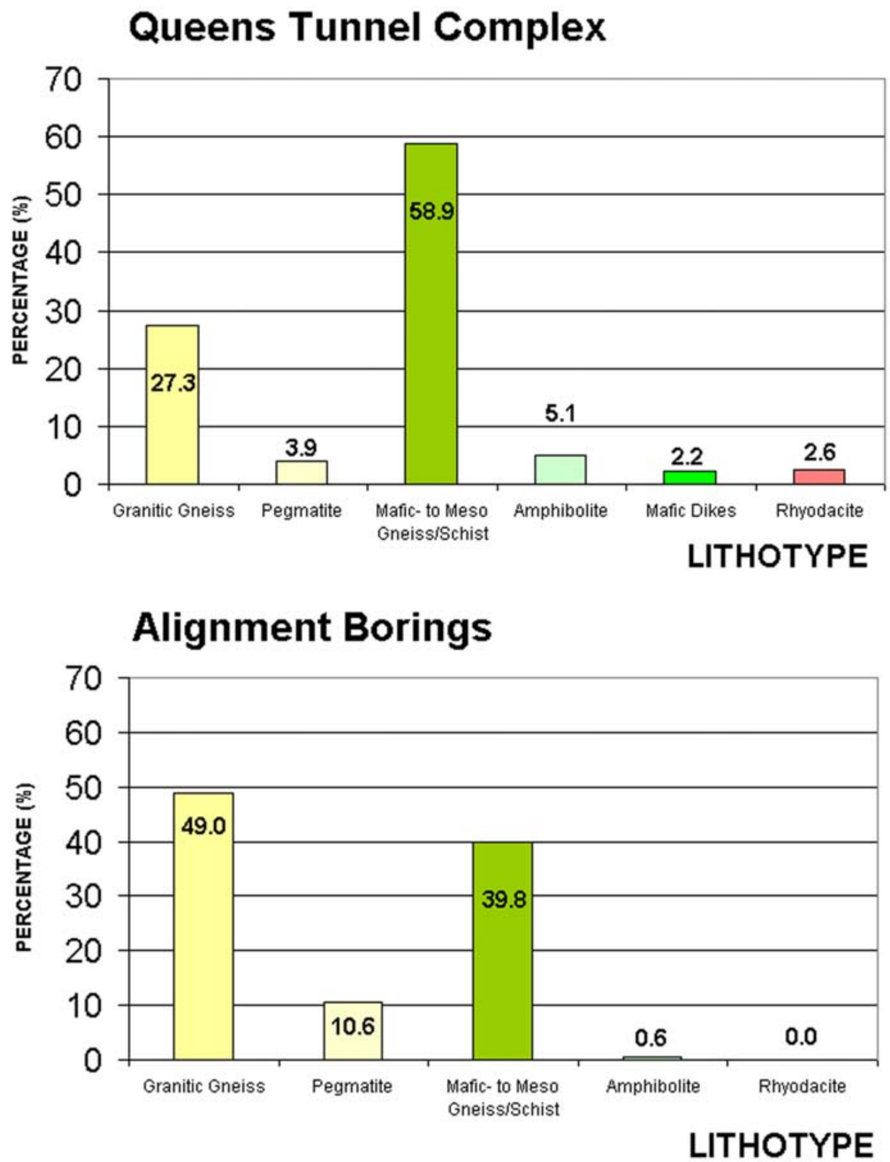

Figure 3 – Bar graphs comparing relative abundances of actual Queens Tunnel lithotypes based on detailed mapping as compared to the expectation from borings.

Grenvillian granulite minerals and fabrics. The oldest fabrics in the Queens Tunnel rocks are medium- to coarse grained, with interlocking plagioclase and pyroxene the primary phases (Figure 4a). Orthopyroxene, a diagnostic indicator of granulite facies metamorphism, is a major or minor component in ~20% of all thin sections examined. Early, coarse-grained garnet coexists with clinopyroxene (cpx) in some rocks and coexists with orthopyroxene (opx) with or without additional cpx in others. The early-stage granulites were extremely anhydrous rocks when first formed. Because of this, the rocks show sparse foliation but exhibit an interlocking granoblastic texture with some light- and dark mineral layering and local "granulite green coloration" at the mesoscopic scale (Brock, Brock and Merguerian 2001).

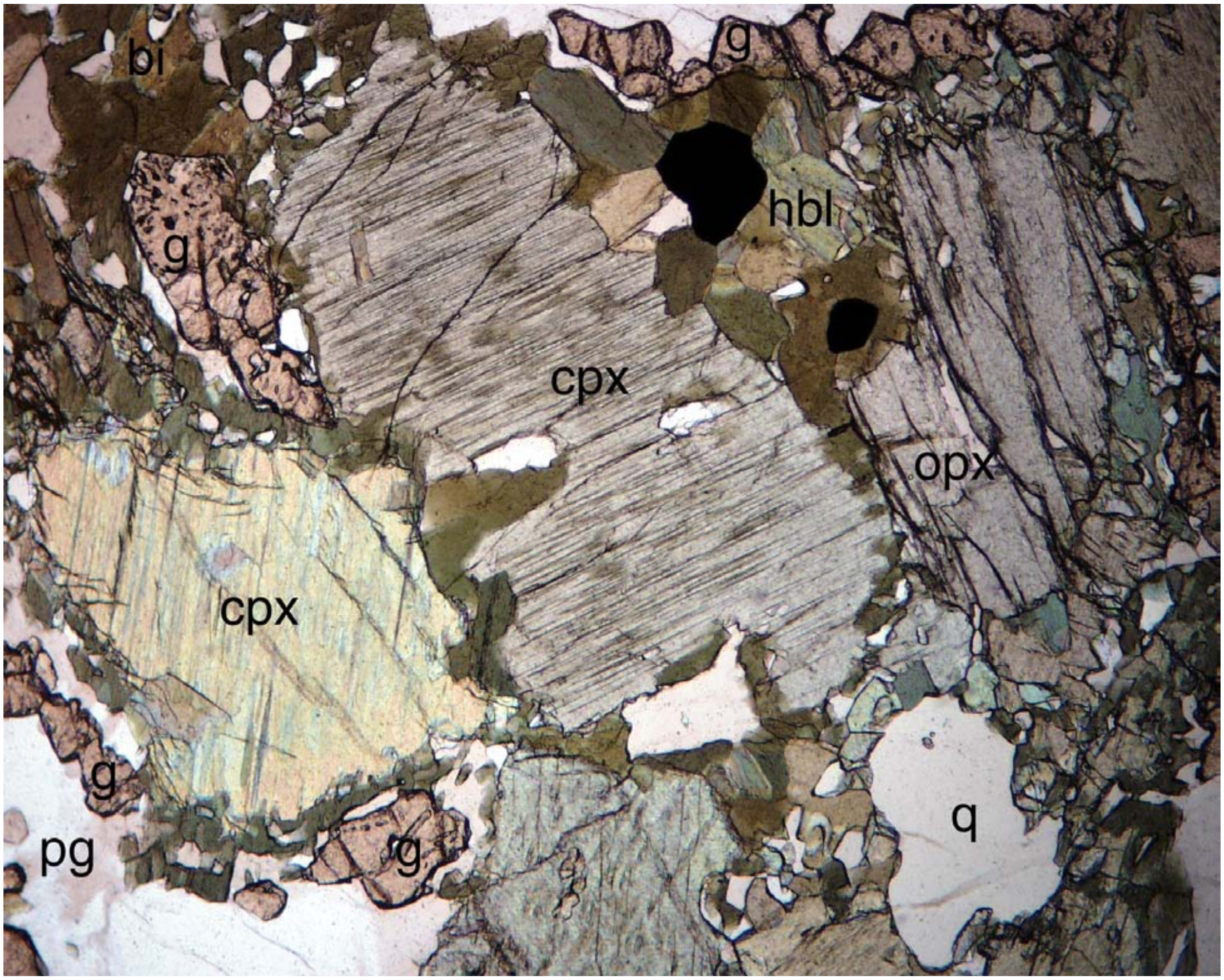

Figure 4a – Photomicrograph in plane-polarized light of Queens Tunnel gneiss showing coarse-grained granulite facies texture in the form of partly recrystallized orthopyroxene (opx), clinopyroxene (cpx), and primary garnet (g). Quartz = q. Note the thin overgrowths of hornblende (hbl), granular garnet (g) and biotite (bi), the result of secondary metamorphic recrystallization. (Sample Q114; Station 15+90; 2 mm field of view.)

Later-stage metamorphism. The "old" Grenvillian pyroxene granulites were subjected to slightly lower grade metamorphism at some later time. The retrogressive reactions occurred under amphibolite- to granulite facies conditions and locally altered the older "primary" granulites with more hydrated mineral assemblages, resulting in the growth of replacement hornblende, cummingtonite, biotite, and recrystallized garnet. Locally, coronas of intergrown amphibole and biotite envelope relict pyroxene. (See Figure 4a.) Late-stage garnet and hornblende occur in nearly complete reaction rims between coexisting orthopyroxene, clinopyroxene, and plagioclase. The recrystallization has produced a distinctive “necklace” texture consisting of granoblastic garnet that stands out in thin section (Figure 4b). These relationships indicate that rocks with “garnet necklace” textures and hornblende probably once contained pyroxene. The early pyroxene granulites tended to survive later-stage metamorphism.

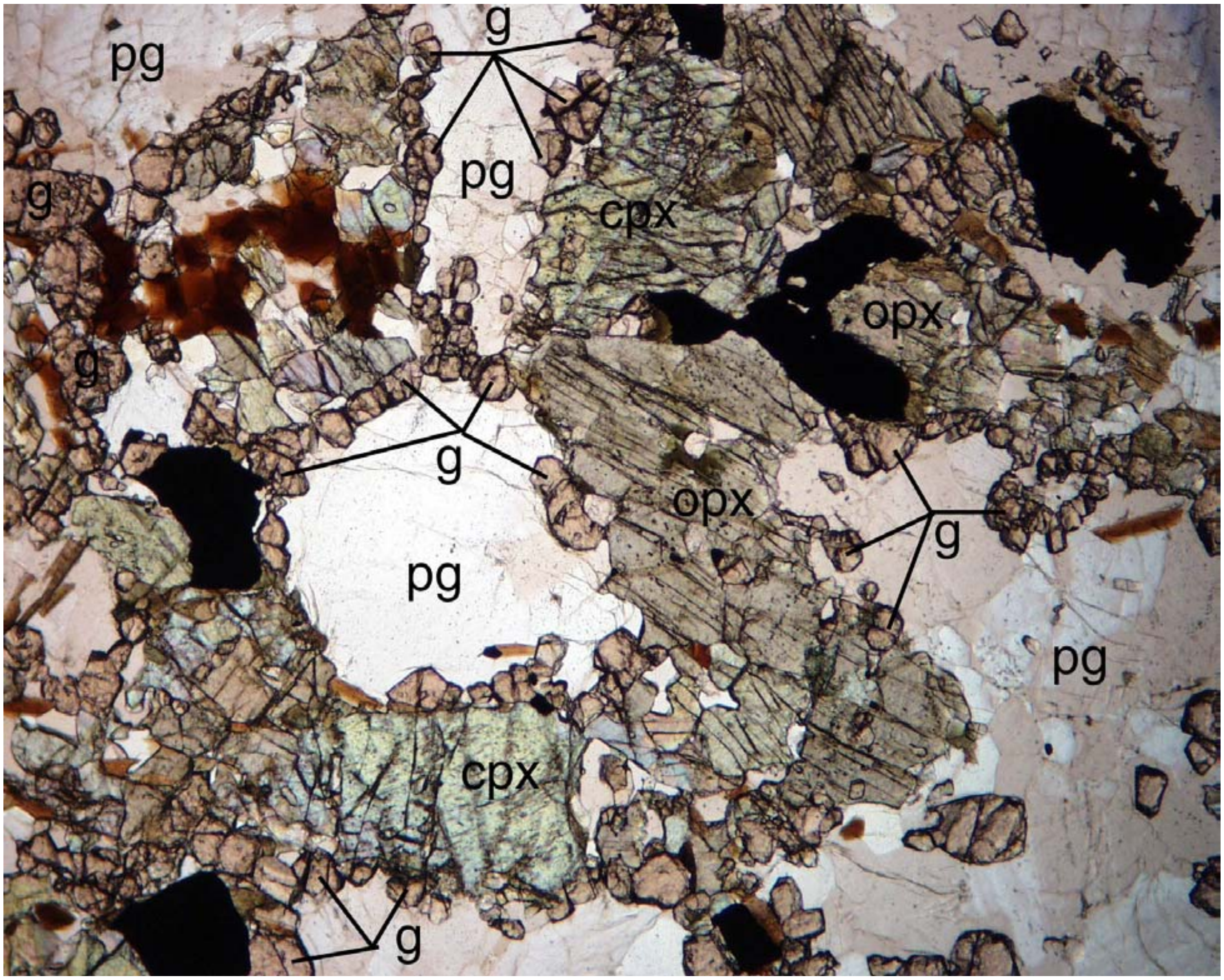

Figure 4b – Photomicrograph in plane-polarized light of Queens Tunnel gneiss showing "garnet necklace" structure. Note the semi-circular patches of high relief garnet. This replacement texture results from the production of garnet and hornblende reactions rims adjacent to primary coarse-grained orthopyroxene, clinopyroxene, and plagioclase during secondary metamorphism. Same notation as above. (Sample Q146; Station 80+64; 2 mm field of view.)

Anomalous Garnet Concentrations. Most petrologists use the term garnetiferous for rocks with roughly 3% to 5% garnet. Based on this definition, nearly the entire tunnel is garnetiferous, yet some areas of the Queens Tunnel are so enriched in garnet (30% to 50%) that the broad use of the qualitative term garnetiferous is misleading. The garnet-enriched zones underlie 10.6% of the Queens Tunnel. Out of 25,127' of as-built Queens Tunnel, over 2,663' are underlain by zones (up to 263' long) of anomalous garnet concentration. Indeed, such garnet concentration might be identified as an "ore deposit" in many parts of the world.

Garnet is sometimes found along with quartz, occurs as disseminated garnet throughout a rock mass, as discrete garnetiferous layers a few feet thick, as lenticular lenses, and in highly laminated zones when sheared. Garnet also occurs in high concentration within amphibole + pyroxene bearing rocks and as garnet + plagioclase segregations. In thin section, aggregates of granular garnet rim areas of relict pyroxene and two garnet growth periods have been recognized. (See Figure 4b.) In the QTC, granulite facies metamorphism promoted the intergrowth of garnet and other dense, anhydrous mineral phases including orthopyroxene and clinopyroxene. During TBM mining the importance of garnet hinges on the extreme hardness of the mineral (Hardness 6.5 to 7.5 on Mohs' scale) and its high density (3.58 to 4.32 g/cm^3). Rocks rich in garnet produce unusually hard, dense, and abrasive rocks. The unusual concentration and high density of garnet has undoubtedly held a first-order impact on the overall density of the QTC.

Garnet-enriched zones presented a special problem to TBM tunneling. Because garnetiferous gneisses are highly recrystallized and granoblastic they are markedly abrasive rocks that adversely effected cutter wear, decreased advance rates, and led to the grinding of rocks and resultant production of excessive fines.

Density Measurements

To better understand the rock mass profile, density (in g/cm^3) was measured from sawn slabs of the Queens Tunnel reference collection of 161 samples. Figure 5 shows the density variation of the samples by station. The graph indicates that the density of the QTC varies from 2.62 to 3.35 and that density decreases toward the higher stations (sloping dark line in Figure 5). Indeed, more mafic lithologies were mapped in the first 18,000' of the tunnel. The mean density of typical granites (2.67 g/cm^3), diorites (2.84 g/cm^3), and gabbros (2.98 g/cm^3) lie within the measured range of QTC values. The density mean of 2.87 g/cm^3 overall defines the QTC as a dioritic (intermediate) rock mass. These measurements are in total accord with lithologic and petrographic examinations that clearly identify garnet-rich intermediate (mesocratic) rocks as the prominent QTC lithotype. (See Figure 3.)

Gneissic Layering

Gneissic rocks exhibit gneissic structure or gneissic layering. Such mineralogic layering results from instability and breakdown of foliation-producing hydrous mineral phases such as mica and amphibole. The AGI glossary states that "in gneisses generally less than 50% of the minerals show preferred orientation". During an initial (Grenvillian) stage of granulite-facies metamorphism, crystallization of pyroxene(s) and plagioclase (+/- garnet) in the QTC, together produced a strong crystalloblastic metamorphic fabric throughout the rock mass. This early granulite metamorphism took place under conditions of extreme temperature and pressure and produced anhydrous mineral assemblages. As a result of their original proto-igneous origin and metamorphic dehydration, many of the rocks of the QTC exhibit coarse layering but little penetrative foliation. The gneissic layering varies from weakly foliated and granoblastic in the interior of massive gneiss bodies to highly foliated and fine-grained in ductile shear zones that cut the gneisses. Both foliated and granoblastic textures are found in the limited areas of metasedimentary rock.

A stereonet analysis of the gneissic layering between Stations 4+00 and 254+00 demonstrated that 26 of 235 poles (11%) indicated subhorizontal layering. Overall 64 poles (27%) show gentle dips. Gently dipping rock fabrics (less than 30°) underlie broad tracts of the Queens Tunnel. Their gentle dips provide a common subhorizontal structural grain in the QTC, an unfavorable rock fabric orientation for efficient TBM mining.

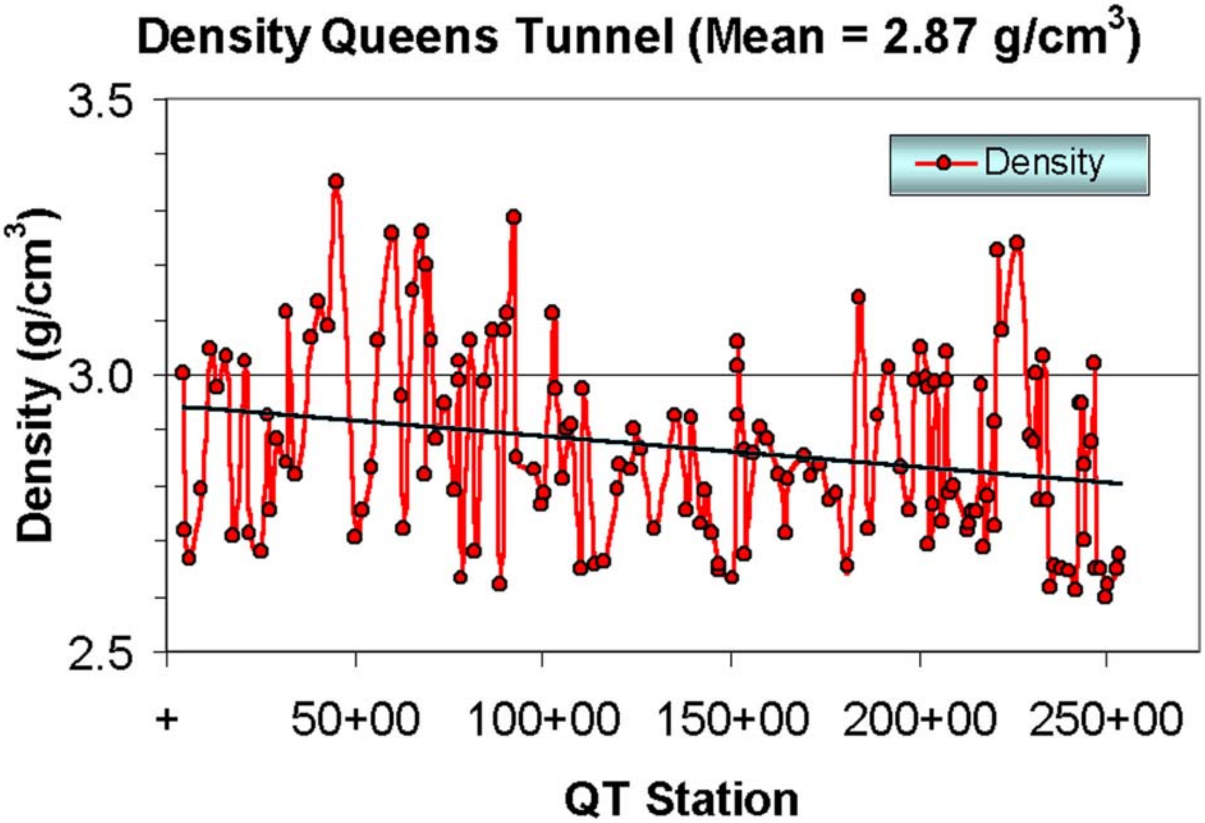

Figure 5 – Rock mass density variation of the Queens Tunnel based on measurement of 161 samples. The rhyodacite dike rocks between Stations 109+20 and 152+40 were not included in the sampling.

Rhyodacite Dikes

Five sub-parallel dikes, all displaying pristine igneous textures, are found in nine formally connected locations in the Queens Tunnel (Merguerian 2001). Although the tunnel boring machine (TBM) may have removed dikes no longer exposed in the tunnel walls, the exposed dike rocks underlie a minimum of 667' between Stations 109+20 and 152+40 and compose 15.4% of the tunnel perimeter rocks within that 4,320' tunnel reach. They occur as tabular, discordant bodies roughly oriented N53°W and average just under 10' in thickness. The larger dikes vary from 16' down to 3' and taper off to thin dikelets. The rhyodacite dikes were injected approximately parallel to a ~N50°W regional fault and fracture pattern but local offshoots of the rhyodacites are sill-like, occurring as small masses that intrude parallel to the existing foliation in the deformed host rocks.

The rhyodacites are reddish, glassy to aphanitic igneous rocks with no metamorphic fabric and low average density (2.58 g/cm^3). Hand samples are hard and flinty in aspect and fresh in appearance with a multitude of curviplanar cooling joints whose intersection produced cobble- to boulder-sized multifaceted blocks and slabs. The dikes, which have yielded preliminary Ar/Ar ages of roughly 295 Ma, crosscut folded Proterozoic Y gneissic rocks of the QTC with which they are clearly genetically and temporally unrelated. The dikes are cut by a generation of steep, NNE-trending brittle faults that are cut by even younger, steep NW- to NNW-trending faults. During TBM mining, a persistent collapsing face, crown, and sidewalls were encountered in the rhyodacite dike areas because of the multitude of smooth cooling joints. Blocky ground consisting of hard, glassy volcanic rock resulted in cutter damage and TBM downtime.

Brittle Faults

Many generations of brittle faults are superimposed on the polydeformed bedrock units of the Queens Tunnel often causing brittle reactivation of ductile faults and pre-existing brittle faults (Merguerian 2002). Over 300 brittle faults were mapped and studied in the Queens Tunnel. They are outlined by fault breccia, clay-rich gouge and are mineralized by quartz, calcite, pyrite, and zeolite minerals. The brittle faults include NW-trending gently SW-dipping faults that commonly reactivate older ductile faults **(Group A)**, younger ENE-trending faults with moderate to steep dips **(Group B)**, subhorizontal faults, reactivated low-angle faults and fractures **(Group C)**, and a steep dip-slip NNE-trending fault set **(Group D)** with thick clay- and zeolite-rich gouge zones (Figure 6). These are all cut by NW- to NNW-trending strike-slip faults of the "Manhattanville" fault set **(Group E)**. Reactivation of older faults is quite common in the tunnel. The two youngest brittle fault sets **(Groups D and E)** cross cut all metamorphic structures and late Paleozoic (295 Ma) glassy rhyodacite dikes. Group E faults have been attributed to neotectonic activity in the Manhattan Prong (Merguerian and Sanders 1996, 1997).

The faults of the Queens Tunnel underlie extended areas of high strain prone to stress relief in the form of joints, invert heave, and rock popping. Joint densities did increase in the vicinity of fault zones but no unique regional joint system was observed to overprint the fault pattern in the tunnel. The faults and joints were parallel and presumed causally related to one another. Local cooling joints in the rhyodacite dikes are not part of the regional joint pattern. In areas of fault convergence, the brittle faults and sub-parallel joints induced detrimental effects on tunneling including a persistent collapsing face, rib and crown fallout, stress relief phenomenon, and local voluminous water inflow.

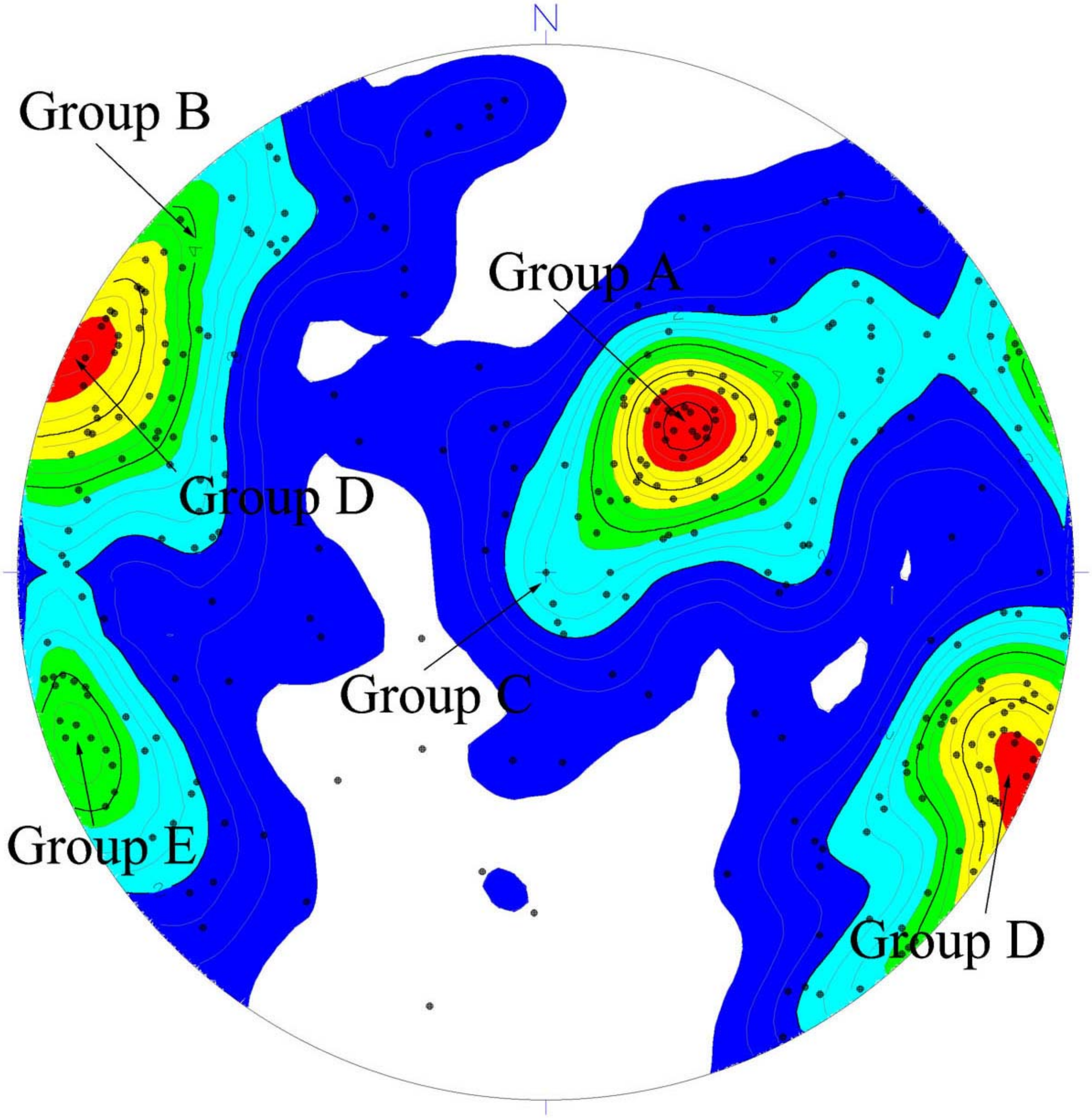

Figure 6 – Contoured Schmidt equal-area stereogram showing the poles to 306 faults mapped in the as-built Queens Tunnel. The older **Group A** faults strike NW and dip gently SW, **Group B** faults are moderate to steep and strike ENE, **Group C** are subhorizontal fractures and faults, **Group D** constitutes a major NNE-trending dip-slip fault system, and **Group E** are the youngest NNW-trending strike-slip faults. Discussion in text.

REDUCED TBM PENETRATION RATE INVESTIGATIONS

The 25,127-ft. long Queens Tunnel was excavated using a 23'2" diameter Robbins main-beam hard rock TBM (Figure 7). This was a high-power machine equipped with 19-inch disc cutters with a rated load capacity of 70 kips per cutter. Table 1 shows the basic specifications of this TBM.

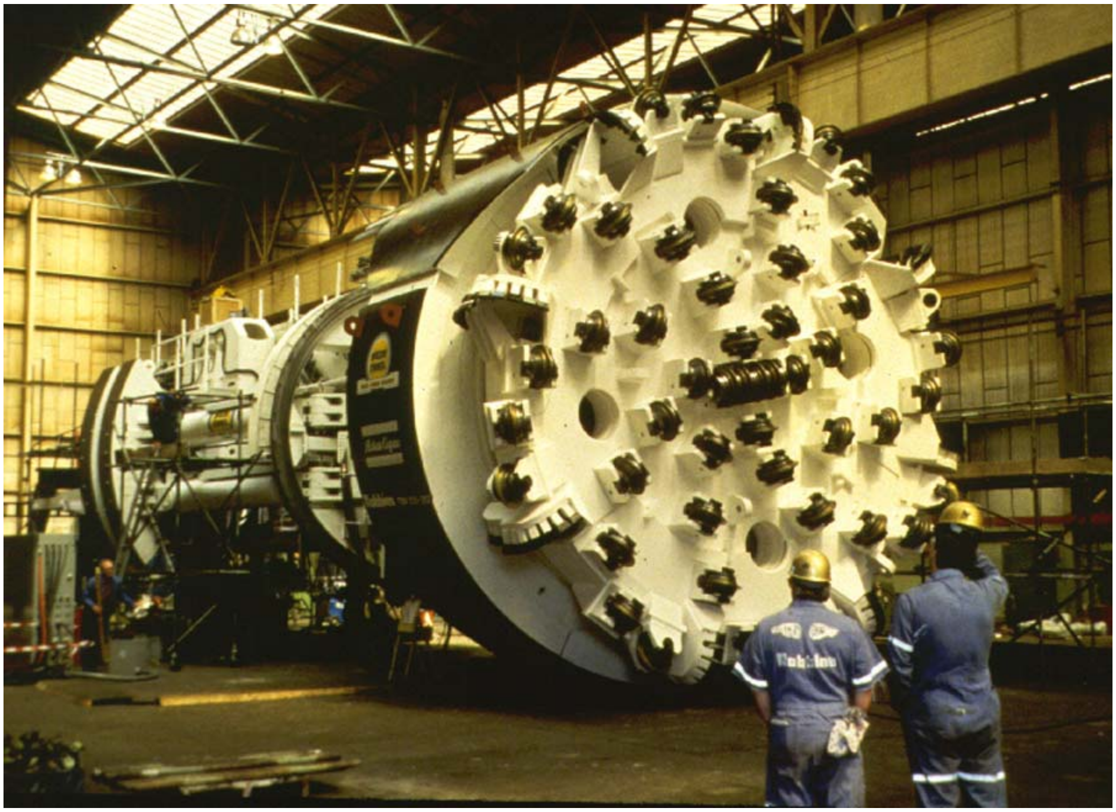

Figure 7 – The front cutterhead and thrust assembly (business-end = 84' length and 23' diameter) of the Queens Tunnel Boring Machine (Robbins Model 235-282). The TBM holed through beneath Long Island City in October 1999 after three years of nearly continuous subsurface mining.

Table 1 - Specifications of Queens Tunnel Boring Machine Model 235–282

Machine Diameter	23’2”
Diameter Range	21’4” to 27’11”
Cutters Number of Disc Cutters Max. Recommended Individual Cutter Load	Series 19 (19”) 50 70,000 lb. (nominal)
Cutterhead Max. Operating Cutterhead Thrust Cutterhead Power Cutterhead Speed Cutterhead Torque Thrust Cylinder stroke	 3,500,000 lbs (nominal) 4220 hp (10x422 hp)* 8.3 RPM 2,669,000 ft-lb 6-ft
Conveyor Capacity (approx.)	650 ft^3/min
TBM Weight (approx.)	640 tons

Based on the analysis of all available pre-bid geotechnical information, the contractor estimated an average penetration rate of about 9.5 ft/hr. for the Robbins machine purchased for the project. The actual penetration rate for the entire tunnel averaged only 6 ft/hr., representing a 35 % reduction from pre-bid estimates. To investigate the cause of this significant penetration loss, an extensive rock testing and TBM performance evaluation program was devised and implemented.

One or more factors could be responsible for the penetration loss experienced in the excavation of the Queens Tunnel. These include overly optimistic pre-bid penetration rate estimates, lower than anticipated cutter loading and harder/tougher rock conditions causing increased difficulty of boring. The investigation program focused on a detailed analysis of these three factors with the principal goal of determining the cause of reduced penetration.

Pre-Bid TBM Performance Estimates

The pre-bid penetration rate estimates developed by the contractor and the machine manufacturer were evaluated and compared with other methods of ROP prediction and the historical data in rocks of similar strength. In addition, a set of predictions was also developed using the CSM predictor model based on the geotechnical information provided pre-bid. All these separate ROP prediction approaches supported the contractor's pre-bid estimate of 9.47 ft/hr.

TBM Cutter Loading

The second issue, which was examined regarding the loss of penetration, was the actual loads imposed on the cutters during mining. The pre-bid TBM performance estimates assume a given cutter load, usually the manufacturer recommended cutter load capacity, for penetration rate calculations. Obviously, if the actual cutter load during operation is below that anticipated, a loss of penetration would occur. The TBM penetration rate is very sensitive to cutter loading and even a slight decrease in cutter load can cause significant reduction in attainable penetration rates during tunnel excavation.

To determine the actual cutter loading during mining, an extensive analysis of machine operational data was performed for the entire tunnel. Fortunately, the Queens TBM was fitted with an on-board automatic data logging system designed to accurately monitor and record all machine operational parameters. The data was recorded in a digital form, which was downloaded directly into a spreadsheet software package for detailed analysis and evaluation. For each machine stroke, the operational parameters were plotted and averages determined. The stroke-based data was also expressed as a function of tunnel station to allow direct comparison of tunnel geology and measured rock properties. Figure 8 shows a typical plot of TBM thrust, stroke and drive motor amps vs. tunnel station.

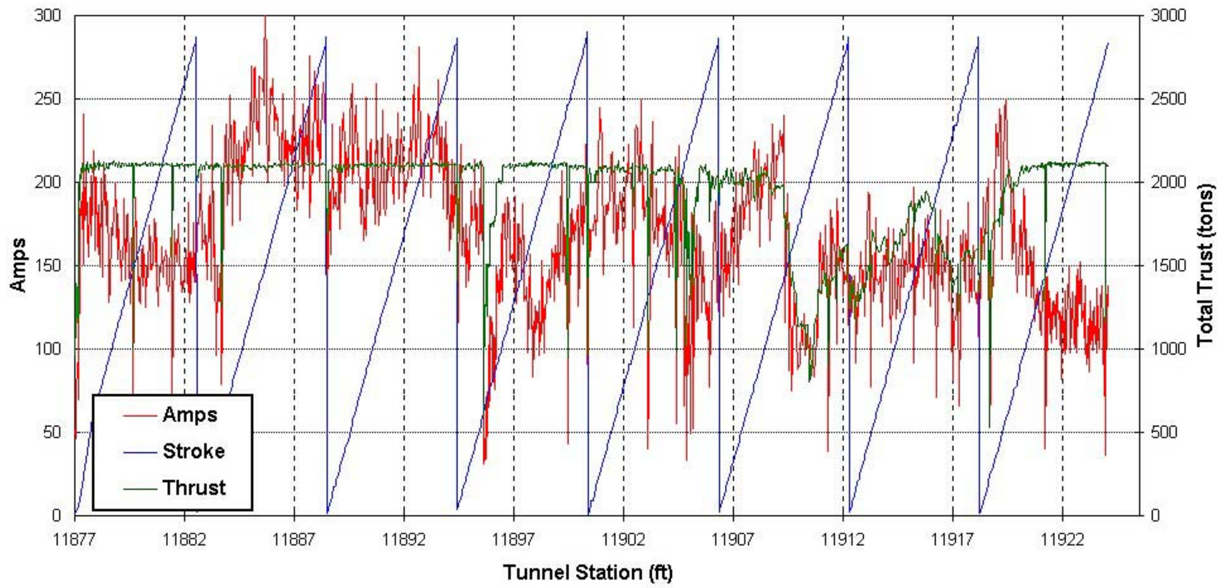

Figure 8 – Raw data plot of machine parameters.

Three separate approaches were used to determine cutter loading from the machine thrust measurements provided by the on-board data acquisition system. Methods 1 and 2 involved the use of net machine thrust and the effective number of cutters. The net thrust is defined as the actual total thrust transmitted to the cutterhead, which is determined by subtracting the machine friction loss and the tow load (as measured by the data logger) from the total thrust generated by the TBM propel system. For Method 1, the frictional loss was assumed to be 5 % of the total thrust. In Method 2, the friction loss was set at 120 tons, which was calculated from a series of no-load field tests carried out on the machine in the tunnel. In Method 3, the cutter load was calculated by simply dividing the total thrust by the total number of cutters on the machine. These three approaches to cutter load determinations resulted in the following values:

Method 1 : 75,472 lbs.
Method 2 : 74,146 lbs.
Method 3 : 72,131 lbs.

The cutter loads from the three separate methods are within 5 % of each cutter. The important point is that they all give values above the 70 kip cutter load value, which was used in developing the pre-bid TBM performance estimates. It should be noted that these cutter loads correspond to the non-blocky ground portions of the tunnel, which made up approximately 19,000 ft. of the total 25,127 ft. length.

To further confirm of the cutter loads calculated from TBM operational data, a set of laboratory cutting tests were also carried out using the CSM Linear Cutting Machine (LCM) in samples of rock retrieved from various locations along the tunnel (Figure 9). These tests were carried out with the new and worn cutters 19-inch cutters actually used on the machine during excavation of the tunnel (Figure 10). LCM tests allow for a very close simulation of field cutting conditions and provide data that can be directly correlated to field TBM performance.

Figure 9 – Linear Cutting Machine.

Figure 10 – View of a 19-inch cutter on LCM.

To compare the LCM-measured cutter forces to those provided by the TBM data logger, the machine data at those tunnel locations where the LCM test samples were retrieved, were also analyzed. At the same penetration, the LCM and the TBM data logger cutter load measurements were as follows:

LCM cutter force measurement	**: 72,120 lbs.**
Field cutter load from TBM data logger	**: 75,920 lbs.**

These cutter load values are very close, within 5 % of each other. This close agreement gives further confirmation that the Queens TBM was operated at cutter loads at or above the manufacturer recommended 70 kip load, which was used in developing the pre-bid ROP predictions. Based on these results, the less than expected cutter loading was also eliminated as a potential cause for the penetration loss experienced in this tunnel.

Harder/Tougher Rock Mass Conditions

The third factor examined for determining the cause of reduced penetration was whether the rock was harder/tougher to excavate than anticipated pre-bid. To address this issue, an extensive tunnel mapping and rock property testing program was formulated and carried out to establish as-built geotechnical specifications for the tunnel. A large number of cores were retrieved at various locations along the tunnel and all rock properties known to influence TBM performance were measured and analyzed. The suite of tests conducted on core samples at each tunnel location sampled included compressive and tensile strength, Cerchar abrasivity index, Punch penetration test, Point load index and thin-section petrographic analysis. In addition, all joints, fractures and rock fabric orientations were mapped in considerable detail along the entire tunnel length as discussed above.

The actual rock compressive strength was found to be about 14 % higher than what was reported pre-bid. This difference was attributed to an insufficient number of tests performed pre-bid. Due to observed rock layering, the tensile strength tests were performed both parallel and perpendicular to the direction of gneissic layering (Figure 11). This approach revealed the impact of gneissic layering on rock tensile strength. The tensile strength across the layering, which corresponds to machine operation when layering is more or less parallel to tunnel axis, was found to be about 38 % higher than along the gneissic layering. Because the strike of gneissic layering encountered in the tunnel was mostly sub-parallel to machine advance, rock chipping efficiency and the TBM performance was adversely impacted.

A battery of Punch Penetration tests were also performed to evaluate the boreability characteristics of the rock formations encountered in the excavation of the Queens tunnel (Figure 12). Punch penetration is the only rock test where the rock surface is actually penetrated by a tool, causing crushing and chipping in a fashion similar to that which occurs with cutters on a TBM. Because this test actually penetrates the rock, it provides the capability to reveal some important rock boreability features that the compressive and the tensile strength tests may fail to show. One important feature which the Punch Penetration test have been successful in identifying is rock toughness which is defined as the resistance of rock to effective chip formation under the cutting action of disc cutters.

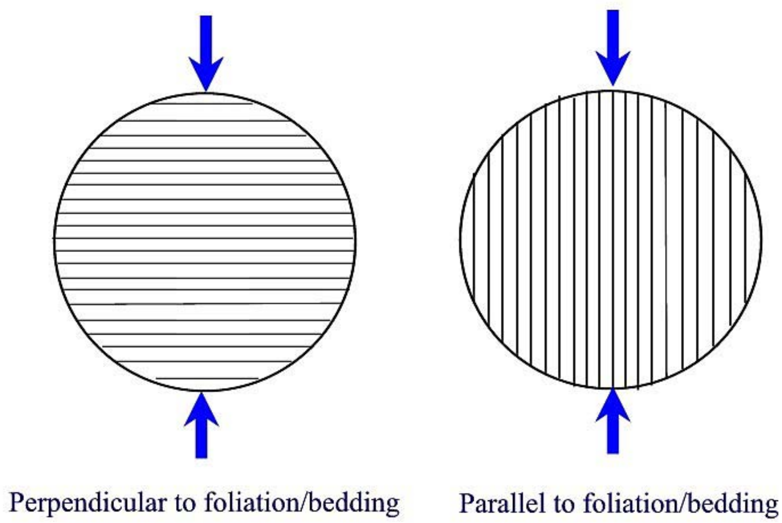

Figure 11 – BTS test set-up and the two directions of loading.

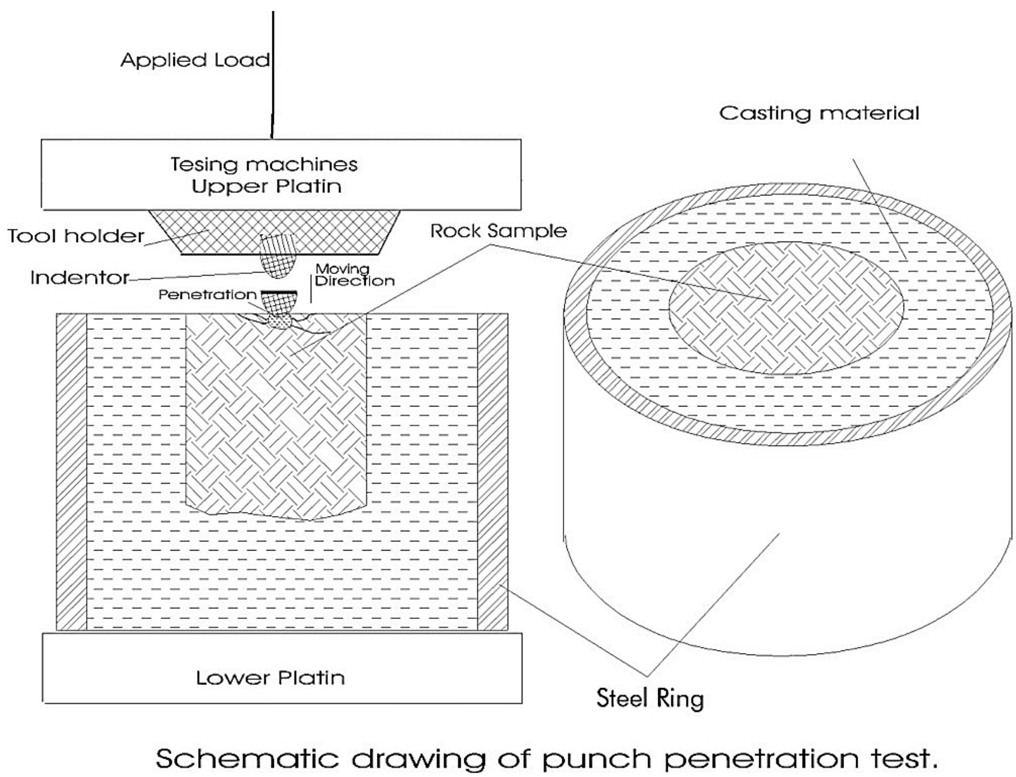

Figure 12 – Punch penetration test set-up.

The Punch Penetration Index for the Queens tunnel was found to be a bout 30 % higher than the standard index for hard rocks. Further, the tests showed that the rock absorbed a high degree of energy prior to chip formation with extensive crushing occurring of the rock beneath the indentor. The high Punch index together with these observations regarding rock failure concluded the existence of a high degree of rock toughness. The encountered Point Load Index (PLI) was found to be about 16 % higher than what was measured pre-bid. Since PLI provides a rough indication of rock strength, the actual values indicate a harder than anticipated rock. We attribute the difficult boreability characteristics of the Queens tunnel rock to the internal fabric of the rock mass, as revealed by thin-section petrography.

CONCLUSIONS

The as-built Queens Tunnel horizon exposes rocks that are clearly not the Paleozoic Hartland Formation. Rather, they are Grenvillian migmatitic gneiss correlative with the Proterozoic Fordham Gneiss. During high-pressure granulite facies metamorphism former plutonic igneous rocks of the Queens Tunnel Complex transformed into dense, coarse- to medium textured orthogneiss consisting of interlocking crystals of plagioclase, pyroxene(s), and primary garnet. A penetrative primary foliation never developed in the QTC because the deep-seated metamorphic conditions precluded the growth of primary hydrous minerals (mica and amphibole), both foliation-producing phases. Rather, a granoblastic texture developed which consisted of interlocking plagioclase and intergrown anhydrous mafic minerals. A second phase of regional metamorphism produced domainal fabrics with localized growth of amphiboles, biotite, and "new" garnet but the "old" granulite textures survived.

Extensive rock testing and TBM performance evaluation studies have provided a correlation between machine performance and natural geologic rock mass properties. The reduced TBM penetration encountered in the construction of the Queens tunnel was caused by higher than anticipated rock strength, adverse direction of rock layering and higher rock toughness brought about by grain interlocking and a high degree of recrystallization, the results of the high-pressure granulite facies metamorphic history.

As a result of the metamorphism the rocks developed zones of unusually pronounced garnet content (at least two growth periods identified). The petrographic analysis also showed that the entire tunnel was garnetiferous with unusual garnet concentrations coupled with a high degree of recrystallization. This created a dense and abrasive rock matrix, also confirmed from Cerchar abrasivity measurements. Together, these textural and mineralogic properties result in rock mass "toughness" and high overall density. Indeed, the gneissic rock mass penetrated in the Queens Tunnel possessed lithologic properties (texture, anhydrous mineralogy, lithology, density, homogeneity, lack of penetrative foliation, and abundant gently dipping fabric orientations) that collectively inhibited efficient TBM mining. We concluded that microscopic rock features produced increased rock toughness resulting in additional loss of penetration. In addition, blocky ground conditions resulted from intersecting fault sets and from fracture patterns unique to a suite of rhyodacite dikes.

The lessons learned from the Queens Tunnel experience include the recognition that a proper GDSR can minimize the pre-bid risks in any subsurface construction effort. As built geological investigations by specialized geologists can define the rock mass conditions and mitigate risks in response to changed conditions. Targeted laboratory testing and machine performance analysis can identify the causes for poor penetration performance.

REFERENCES

Baskerville, C. A., 1989, New York City: juxtaposition of Cambrian and Ordovician miogeoclinal and eugeoclinal rocks: p. T361:39-T361:48 *in* Baskerville, C. A. *ed*., Geology and engineering geology of the New York Metropolitan area, International Geological Congress, 28th, Washington, D. C., Guidebook to Field Trip T361, 59 p.

Baskerville, C. A., 1992, Bedrock and engineering geologic maps of Bronx County and parts of New York and Queens counties, New York: U. S. Geological Survey Miscellaneous Investigations Series Map I-2003 (2 sheets; colored maps on scale of 1/24,000).

Baskerville, C. A., 1994, Bedrock and engineering geology maps of New York County and parts of Kings and Queens counties, New York and parts of Bergen and Hudson counties, New Jersey: U. S. Geological Survey Miscellaneous Investigations Series Map I-2306 (2 sheets; colored maps on scale of 1/24,000).

Baskerville, C. A.; and Mose, D., 1989, The separation of the Hartland formation and the Ravenswood granodiorite from the Fordham gneiss at Cameron's Line in the New York City area: Northeastern Geology, v. 11, p. 22-28.

Berkey, C. P., 1910, Areal (*sic*) and structural geology of southern Manhattan Island: New York Academy of Sciences Annals, v. 19, no. 11, part 2, p. 247-282.

Berkey, C. P., 1933, Engineering geology of the City of New York, p. 77-123 *in* Berkey, C. P., *ed*., Guidebook 9, New York Excursions, New York City and vicinity: International Geological Congress, 16th, United States, 1933, Washington, D. C., United States Government Printing Office, 151 p.

Berkey, C. P., 1948, Engineering geology in New York City, Excursion No. 4, p. 51-66 *in* Creagh, Agnes, *ed*., Guidebook of Excursions: Geological Society of America Annual Meeting, 61st, New York City, 135 p.

Berkey, C. P.; and Fluhr, T. W., 1948, Engineering geology of New York City water supply, Excursion No. 12, p. 121-135 *in* Creagh, Agnes, *ed*., Geological Society of America, 61st Annual Meeting, New York City, Guidebook of Excursions, 135 p.

Blank, H. R., 1973, Observations on the Brooklyn injection gneiss and related formations: New York Academy of Sciences Transactions, series II, v. 35, no. 8, p. 645-660.

Brock, Pamela Chase; Brock, Patrick W. G.; and Merguerian, Charles, 2001, The Queens Tunnel Complex: a newly discovered granulite facies Fordham orthogneiss complex that dominates the subsurface of western Queens: p. 1-8 *in* Hanson, G. N., *chm*., Eighth Annual Conference on Geology of Long Island and Metropolitan New York, 21 April 2001, State University of New York at Stony Brook, NY, Long Island Geologists Program with Abstracts, 128 p.

Clark, S. P. Jr. (ed.), 1966, Handbook of Physical Constants: Geological Society of America Memoir 97, 587 p.

Fisher, D. W., Isachsen, I. W., and Rickard, L. V., *editors and compilers*, 1970, Geological map of New York: New York State Museum and Science Service Map and Chart Series Number 15, scale 1/250,000.

Hatch, N. L., Jr.; and Stanley, R. S., 1973, Some suggested stratigraphic relations (*sic*) in part of southwestern New England: United States Geological Survey Bulletin 1380, 83 p.

Merguerian, Charles, 1983, Tectonic significance of Cameron's Line in the vicinity of the Hodges Complex--an imbricate thrust model for Western Connecticut: American Journal of Science, v. 283, p. 341-368.

Merguerian, Charles, 1996, Stratigraphy, structural geology, and ductile- and brittle faults of New York City, p. 53-77 *in* Benimoff, A. I. and Ohan A. A., *chm.*, The Geology of New York City and Vicinity, Field guide and Proceedings, New York State Geological Association, 68th Annual Meeting, Staten Island, NY, 178 p.

Merguerian, Charles, 1999a, The Bedrock Geology of the Queens Tunnel: Duke Geological Laboratory Report QT9906, 109 p. + Geological Map Portfolio, Scale 1"=10' (Stations 96+00 to 156+00).

Merguerian, Charles, 1999b, Techniques of TBM tunnel mapping - the Queens Tunnel, NYC, p. 8-12 *in* Hanson, G. N., *chm*., Sixth Annual Conference on Geology of Long Island and Metropolitan New York, 24 April 1999, State University of New York at Stony Brook, NY, Long Island Geologists Program with Abstracts, 143 p.

Merguerian, Charles, 2000, Rock mass properties of the Queens Tunnel Complex: Duke Geological Laboratory Report QT0010, 257 p. + Geological Field Map Album, Scale 1"=10' (Stations 3+65 to 254+00).

Merguerian, Charles, 2001, Young rhyodacite dikes found in the Queens Tunnel, beneath Woodside, Queens: p. 9-19 *in* Hanson, G. N., *chm*., Eighth Annual Conference on Geology of Long Island and metropolitan New York, 21 April 2001, State University of New York at Stony Brook, NY, Long Island Geologists Program with Abstracts, 128 p.

Merguerian, Charles, 2002, Brittle Faults of the Queens Tunnel Complex, NYC Water Tunnel #3: p. 63-73 *in* Hanson, G. N., *chm*., Ninth Annual Conference on Geology of Long Island and metropolitan New York, 20 April 2002, State University of New York at Stony Brook, NY, Long Island Geologists Program with Abstracts, 116 p.

Merguerian, Charles; Brock, Pamela Chase; and Brock, Patrick W. G., 2001, The Queens Tunnel Complex – a granulite facies orthogneiss terrane exposed in NYC Water Tunnel #3 (abs.): Geological Society of America Abstracts with Programs, v. 33, no. 6, p. A46.

Merguerian, Charles; and Sanders, J. E., 1991b, Geology of Manhattan and the Bronx: Guidebook for On-The-Rocks 1990-91 Fieldtrip Series, Trip 16, 21 April 1991, Section of Geological Sciences, New York Academy of Sciences, 141 p.

Merguerian, Charles; and Sanders, J. E., 1993d, Geology of southern Central Park, New York City: Guidebook for On-The-Rocks 1993 Fieldtrip Series, Trip 28, 26 September 1993, Section of Geological Sciences, New York Academy of Sciences, 143 p.

Merguerian, Charles; and Sanders, J. E., 1996, Diversion of the Bronx River in New York City - evidence for postglacial surface faulting?, p. 131-145 *in* Hanson, G. N., *chm*., Geology of Long Island and metropolitan New York, 20 April 1996, State University of New York at Stony Brook, NY, Long Island Geologists Program with Abstracts, 177 p.

Merguerian, Charles; and Sanders, J. E., 1997, Bronx River diversion: neotectonic implications (abs.): Paper No. 198, p. 710 *in* Hudson, J. A. and Kim, Kunsoo, *eds.*, International Journal of Rock Mechanics and Mining Sciences, Special Issue, 36th U.S. Rock Mechanics Symposium, Columbia University, New York, June 29-July 02, 1997, v. 34, no. 3/4, 714 p. Full version on CD-ROM, 10 p.

Merrill, F. J. H., and others, 1902, Metamorphic crystalline rocks of the New York City quadrangle, *in* Merrill, F. J. H.; Darton, N. H.; Hollick, Arthur; Salisbury, R. D.; Dodge, R. E.; Willis, Bailey; and Pressey, H. A., Description of the New York City district: United States Geological Survey Geologic Atlas of the United States, New York City Folio, No. 83, 19 p. (Includes colored geologic map on a scale of 1:62,500).

Rodgers, John; Gates, R. M.; and Rosenfeld, J. L., 1959, Explanatory text for the preliminary geological map of Connecticut, 1956: Connecticut Geological and Natural History Survey Bulletin 84, 64 p.

Rodgers, John, 1985, Bedrock geological map of Connecticut: Hartford, CT, Connecticut Geological and Natural History Survey, Connecticut Natural Resources Atlas Series, scale 1:250,000.

Spear, F. S., 1993, Metamorphic phase equilibria and pressure-temperature-time paths: Mineralogical Society of America Monograph, Mineralogical Society of America, Washington, D. C., 799 p.

Filename: CMLO2003.html